

High-Temperature Superconductivity in Single-Unit-Cell FeSe Films on Anatase TiO₂(001)

Hao Ding,¹ Yan-Feng Lv,¹ Kun Zhao,¹ Wen-Lin Wang,¹ Lili Wang,^{1,2}
Can-Li Song,^{1,2} Xi Chen,^{1,2} Xu-Cun Ma,^{1,2} and Qi-Kun Xue^{1,2,*}

¹*State Key Laboratory of Low-Dimensional Quantum Physics,
Department of Physics, Tsinghua University, Beijing 100084, China*

²*Collaborative Innovation Center of Quantum Matter, Beijing 100084, China*

We report on the observation of high-temperature (T_c) superconductivity and magnetic vortices in single-unit-cell FeSe films on anatase TiO₂(001) substrate by using scanning tunneling microscopy. A systematic study and engineering of interfacial properties has clarified the essential roles of substrate in realizing the high- T_c superconductivity, probably via interface-induced electron-phonon coupling enhancement and charge transfer. By visualizing and tuning the oxygen vacancies at the interface, we find their very limited effect on the superconductivity, which excludes interfacial oxygen vacancies as the primary source for charge transfer between the substrate and FeSe films. Our findings have placed severe constraints on any microscopic model for the high- T_c superconductivity in FeSe-related heterostructures.

PACS numbers: 74.70.Xa, 68.37.Ef, 74.62.Dh, 74.25.Uv

The recent discovery of superconductivity with an exceptionally high critical temperature (T_c) over 65 K in single-unit-cell (SUC) FeSe films on SrTiO₃ has received extensive attention [1–10]. Distinct from iron pnictide and bulk FeSe compounds [11, 12], the superconducting SUC FeSe films prepared on SrTiO₃ substrate not only possess a rather simple Fermi surface topology—only having electron pockets around the zone corner (M point) of Brillouin zone Fermi surface (E_F) [2, 4, 7], but also reach a record of T_c values among all iron-based superconductors (Fe-SCs) [1–4]. In order to understand the enhancement in T_c , several different scenarios invoking interface effects, such as interfacial electron-phonon coupling [1, 7, 9, 10], charge transfer prompted by interfacial oxygen vacancies [2–4, 6], tensile strain effect induced by the lattice mismatch between FeSe and SrTiO₃ [4, 13], screening effect by SrTiO₃ ferroelectric phonons [5], have been proposed. However, a consensus on which factors play the primary roles in enhancing the superconductivity of FeSe has not yet been achieved. The situation is further complicated by the observation of high- T_c superconductivity in anisotropic SrTiO₃(110) substrates [14, 15] and heavily electron-doped FeSe-derived superconductors involving little interfacial effect [16–20].

Attempt to separate the effects of substrate by preparing FeSe films on graphitized SiC(0001) leads to the discovery of two disconnected superconducting domes upon alkali-metal potassium doping [19]: a low- T_c phase in undoped parent FeSe and a high- T_c phase in heavily electron-doped regime. This points out a different pairing mechanism of high- T_c phase from that in other Fe-SCs. Most importantly, the observed T_c of ~ 48 K and Δ of ~ 14 meV in these systems [16, 17, 19, 20] imply that, to boost the higher T_c in FeSe [1–4], the SrTiO₃ must impose additional effect(s) other than the electron doping.

In order to clarify the above-mentioned controversies, it is highly desirable to find an alternative substrate that can host high- T_c superconductivity and meanwhile allow a straightforward comparison with SrTiO₃.

Realizing that the SrTiO₃ substrates commonly have a termination of TiO₂ under ultrahigh vacuum (UHV) preparation conditions, we grow anatase TiO₂ directly on SrTiO₃ as substrate for FeSe growth by molecular beam epitaxy (MBE). The epitaxial anatase TiO₂ with various distinctive physical properties from SrTiO₃ allows for a direct scrutiny of interfacial effects on the emerging high- T_c superconductivity.

Our experiments were conducted in a Unisoku UHV scanning tunneling microscopy (STM) system, equipped with a MBE chamber for film preparation. The base pressure is better than 1.0×10^{-10} Torr. The 0.05 wt Nb-doped SrTiO₃(001) substrates were degassed at 600°C for 3 hours, and then annealed at 1250°C for 20 minutes to get clean and flat surface. Anatase TiO₂ islands were grown on SrTiO₃(001) at 750°C by evaporating high-purity Ti (99.99%). At this temperature, oxygen atoms decompose from SrTiO₃ and react with the deposited Ti to form anatase TiO₂. The growth rate was approximately 0.11 monolayers per minute, which was calibrated by STM. FeSe films were then grown on anatase TiO₂(001) surface at 500°C by co-evaporating high-purity Fe (99.995%) and Se (99.999%) from standard Knudsen cells under Se-rich condition. The growth rate was ~ 0.01 layers per minute. With the growth recipe, the as-grown SUC FeSe films on anatase TiO₂(001) are superconducting without need of post-growth annealing. All STM images were acquired at 4.2 K with a polycrystalline PtIr tip. The dI/dV spectra were acquired using lock-in technique with a bias modulation of 10 mV and 0.5 mV for wide-energy-scale (-0.5 V \sim 0.5 V) and

small-energy-scale (-50 mV \sim 50 mV) spectra at 913 Hz, respectively.

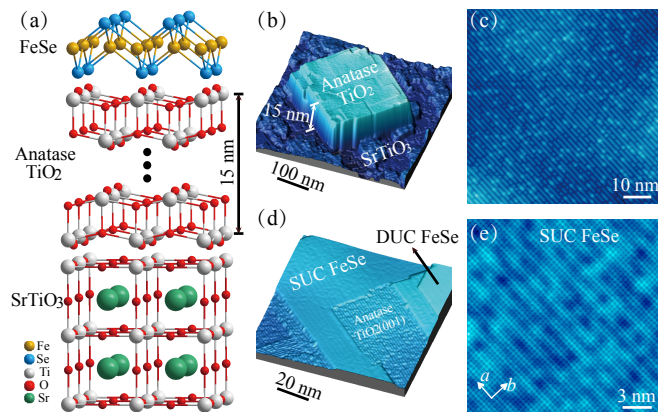


FIG. 1. (color online) (a) Schematic of FeSe/TiO₂(001) heterostructure. The surface reconstructions of SrTiO₃(001) and anatase TiO₂(001) are not shown for clarity. For the typical TiO₂(001) thick films studied, its in-plane lattice constant has been well relaxed to 0.380 nm from 0.3905 nm. (b) STM topography (500 nm \times 500 nm, $V_s = 3.0$ V, $I_t = 0.03$ nA) showing an anatase TiO₂(001) island with a thickness of 15 nm supported by a SrTiO₃(001) substrate. (c) Zoom-in STM topography (70 nm \times 70 nm, $V_s = 1.5$ V, $I_t = 0.03$ nA) acquired on a TiO₂ island, showing clear 4×1 reconstruction plus oxygen vacancies (bright spots). (d) STM topography (100 nm \times 100 nm, $V_s = 3.0$ V, $I_t = 0.03$ nA) showing co-existing SUC and DUC FeSe films on anatase TiO₂(001). (e) Atomically resolved STM topography (20 nm \times 20 nm, $V_s = 50$ mV, $I_t = 0.1$ nA) of SUC FeSe film. *a* and *b* correspond to either of Se-Se nearest-neighbor directions throughout.

As sketched in Fig. 1(a), anatase TiO₂ is characterized with distinct O-Ti-O triple-layered planes in sharp contrast to the single-layered TiO₂ planes in SrTiO₃. This has consequently led to a great deal of diversities between their physical properties such as lattice constants, phonon modes and dielectric constants. The in-plane lattice constant of anatase TiO₂(001) is 0.3782 nm, much closer to that (0.3765 nm) of FeSe than that (0.3905 nm) of SrTiO₃(001). Distinct from a ferroelectric soft phonon mode with a frequency of 88 cm⁻¹ in SrTiO₃, which has been proposed to be crucial for the T_c enhancement in SUC FeSe/SrTiO₃ [5], the corresponding phonons in anatase TiO₂ have a quite high frequency (367 cm⁻¹) and a very limited contribution to static dielectric constant (22.7 along the *c*-axis, significantly smaller than 300 of SrTiO₃) [21]. As thus, the anatase TiO₂(001) serves as an advisory system to distinguish whether or not the above-mentioned parameters bear a primary responsibility for the enhanced high- T_c superconductivity in FeSe-related heterostructures. Furthermore, in contrast with SrTiO₃ where the oxygen vacancies have never been directly identified [1, 14, 15], oxygen vacancies on anatase TiO₂ can be easily tuned in their density by annealing [22] and visualized by STM. This renders anatase TiO₂

a unique substrate for a systematic study of the role of oxygen vacancies in the superconductivity of SUC FeSe.

The as-grown samples exhibit isolated TiO₂ islands with a typical thickness of 15 nm and a lateral size as large as 300 nm \times 300 nm on SrTiO₃(001) [Fig. 1(b)]. Figure 1(c) depicts a zoom-in image of TiO₂(001) island, which clearly reveals the well-known 4×1 reconstruction decorated by some oxygen vacancies (bright spots) [22]. After a precise calibration of our STM piezotube scanner, the in-plane lattice constant is measured to be 0.380 ± 0.005 nm (close to the value of 0.3782 nm in bulk TiO₂), indicative of a nearly fully relaxed lattice. On the substrate with the unstrained anatase TiO₂(001) islands, we then grow FeSe films using the previously established method [1, 12], which leads to formation of atomically flat SUC and double-unit-cell (DUC) films with very few defects [Figs. 1(d) and 1(e)]. Our subsequent STM measurements reveal the same in-plane lattice constant of both SUC and DUC FeSe as TiO₂, 0.380 ± 0.005 nm, slightly larger than the value (0.3765 nm) of bulk FeSe within the experimental uncertainty. The result suggests nearly strain-free FeSe films formed on anatase TiO₂(001), resembling with those on graphene/SiC(0001) [12, 19].

Tunneling conductance dI/dV spectrum on SUC (red curve) and DUC (magenta curve) FeSe films on anatase TiO₂(001) are illustrated in Fig. 2(a), which behave very differently. Although the overall feature on DUC resembles more closely with undoped parent FeSe (black curve), the dI/dV spectrum on SUC differs markedly from both, but bears great similarities with those acquired in SUC FeSe films on SrTiO₃ (blue curve) and in K-doped FeSe films [19]. The result reveals a substantial electron transfer from anatase TiO₂(001) to SUC FeSe film. Subsequent dI/dV measurements in a smaller energy scale [Figs. 2(b) and 2(c)] reveal first evidence of superconductivity as SUC FeSe/SrTiO₃: spatially rather universal and U-shaped gaps with vanishing density of states near the Fermi energy (E_F). The double-gap (denoted as Δ_1 and Δ_2 , respectively) structure most probably suggests a multi-band superconductor [20, 23]. The maximal gap Δ_1 varies from 17 meV [Fig. 2(b)] to 21 meV [Fig. 2(c)], even slightly larger than those measured in SUC FeSe/SrTiO₃ films [1–4, 7, 23]. This might mean a higher T_c in SUC FeSe/TiO₂ films, which merits a further study of the temperature-dependent superconducting gap in the future. Note that the DUC FeSe films on TiO₂(001) exhibit no superconductivity signature at all [Fig. 2(c)], resembling with the DUC FeSe films on SrTiO₃ [1]. This may be caused by a small amount of but insufficient electron transfer from TiO₂ to DUC FeSe films, which pushes them to the nonsuperconducting region between the recently discovered two superconducting domes of FeSe [19].

To confirm that the gap opening around E_F observed in Figs. 2(b) and 2(c) is related to superconductivity,

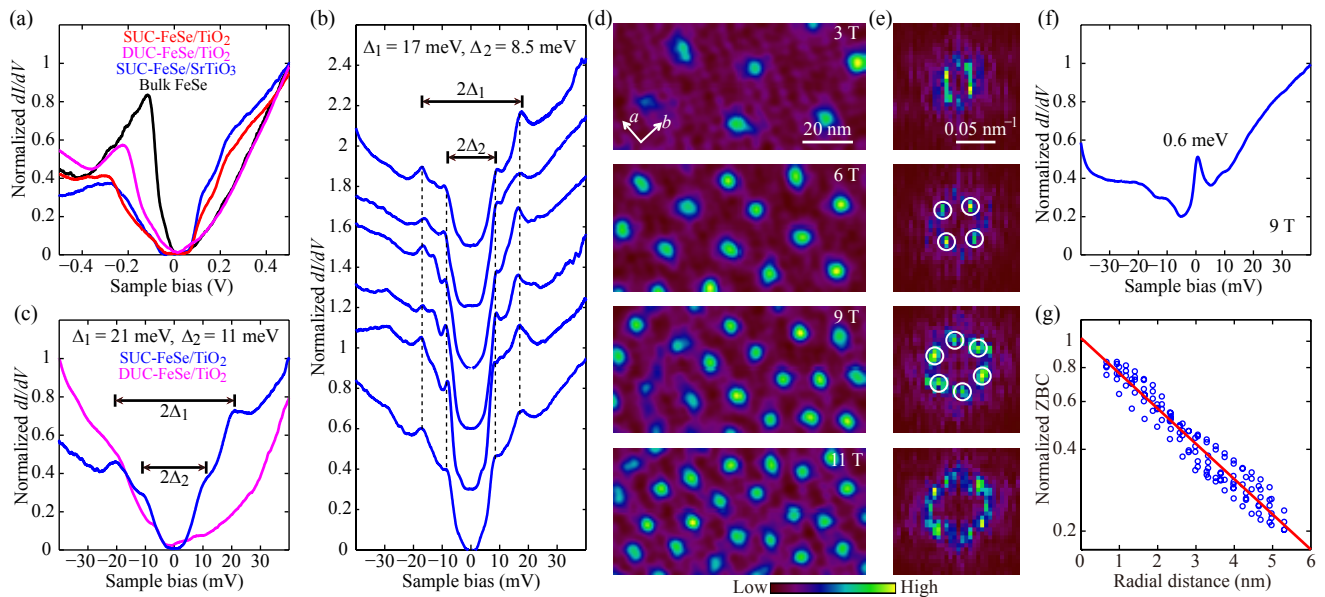


FIG. 2. (color online) (a) Comparison of large-energy-scale dI/dV spectra (set point: $V_s = 0.5$ V, $I_t = 0.1$ nA) of FeSe films on anatase $\text{TiO}_2(001)$ (red and magenta curves) and $\text{SrTiO}_3(001)$ (blue curve), as well as undoped bulk FeSe (black curve). (b, c) Low energy dI/dV spectra (set point: $V_s = 50$ mV, $I_t = 0.4$ nA) taken on various SUC FeSe/ $\text{TiO}_2(001)$ films (blue curves) revealing the typical and largest superconducting gap, respectively. Vertical dashes are guide to eye. The spectrum color-coded by magenta in c indicates no superconductivity on DUC FeSe films. (d) ZBC map (100 nm \times 50 nm, set point: $V_s = 50$ mV, $I_t = 0.1$ nA) showing the vortices under various magnetic fields in SUC FeSe/ $\text{TiO}_2(001)$. Yellow regions with enhanced ZBC, due to the suppressed superconducting gap, indicate the individual isolated vortices. (e) FFT power spectra of the ZBC maps in d. (f) Differential conductance dI/dV spectrum (set point: $V_s = 50$ mV, $I_t = 0.4$ nA) measured at a vortex center at 9 T, showing the suppressed superconductivity and Andreev bound states at 0.6 meV. (g) Radial dependence of normalized ZBC around a single vortex core (blue circles). The fit to an exponential decay (red line), namely $\text{ZBC}(r) = g_0(x = \infty) + A\exp(-r/\xi_{\text{GL}})$ with $g_0(x = \infty)$ as the constant background, leads to an angularly averaged GL coherence length $\xi_{\text{GL}} = 2.85 \pm 0.14$ nm. The normalized dI/dV spectrum was obtained by dividing the raw one by its conductivity value at the tunneling set point.

we have conducted varying magnetic field experiment. Application of magnetic field perpendicular to a superconducting SUC FeSe/ $\text{TiO}_2(001)$ films can suppress its local superconductivity, leading to the formation of vortices and Abrikosov lattice. This situation is demonstrated by the zero-bias conductance maps in Fig. 2(d). The magnetic vortices, seen as zero-bias conductance enhancement, increase linearly in number with the field B , as anticipated. Remarkably a nearly square vortex lattice, more clearly seen in fast Fourier-transferred (FFT) images in Fig. 2(e), is observable at $B = 6$ T. This supports a fourfold anisotropy in the superconducting order parameter [24–26], bearing a strong likeness to the moderately anisotropic gap in SUC FeSe/ SrTiO_3 films measured by a recent angle-resolved photoemission spectroscopy experiment [20]. Based on this model, the gap minima should be located along the nearest-neighbor directions of the square vortex lattice, which is orientated along the Se-Se bond directions [Fig. 2(d)]. This observation puts strong constraints on the electron pairing symmetry in SUC FeSe/ $\text{TiO}_2(001)$ films. At 9 T, the vortices change into a distorted triangle lattice. Such evolution of vortex structure has previously been found in $\text{YNi}_2\text{B}_2\text{C}$ [27], high- T_c cuprate $\text{La}_{1.83}\text{Sr}_{0.17}\text{CuO}_4$ [28] and CeCoIn_5

[29], which might be caused by other competing effects, such as Fermi surface anisotropy [30].

In the vicinity of vortex core, our dI/dV measurements reveal the presence of an Andreev bound state at $E_0 = 0.6$ meV linking with lowest bound state [31] and the complete disappearance of double-superconducting-gap structure [Fig. 2(f)]. The results demonstrate unambiguously the gaps as superconducting gaps as well as the occurrence of high- T_c superconductivity in SUC FeSe/ $\text{TiO}_2(001)$ films. Analysis of the spatial evolution of radial zero-bias-conductance (ZBC) values around the vicinity of vortices [Fig. 2(g)] has led to a Ginzburg-Landau (GL) coherence length $\xi_{\text{GL}} = 2.85 \pm 0.14$ nm, consistent with that ($2.45 \sim 3.18$ nm) of SUC FeSe/ SrTiO_3 films [23]. The observed particle-hole asymmetry at the vortex core with the lowest bound state on the empty state [Fig. 2(f)] indicates electron-type charge carriers in superconducting SUC FeSe/ $\text{TiO}_2(001)$ [31], in good agreement with the dI/dV measurements above [Fig. 2(a)].

Our demonstration of superconductivity with a very large Δ in the SUC FeSe films on TiO_2 constitutes a critical finding related to the interfacial high- T_c superconductivity. The finding, that Δ appears larger than those (8

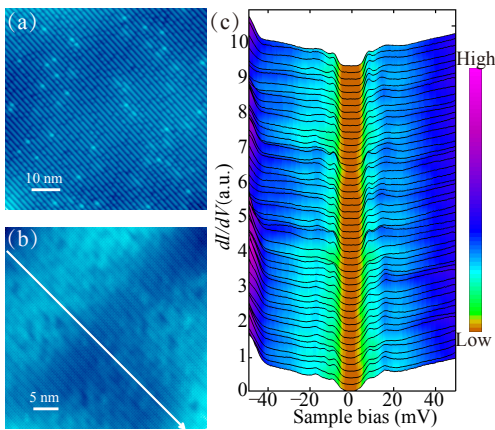


FIG. 3. (color online) (a) STM topography ($70 \text{ nm} \times 70 \text{ nm}$, $V_s = 1.0 \text{ V}$, $I_t = 0.03 \text{ nA}$) of anatase $\text{TiO}_2(001)$ with significantly lower density of oxygen vacancies after post-growth annealing at 750°C . (b) Atomically resolved STM topography ($40 \text{ nm} \times 40 \text{ nm}$, $V_s = -50 \text{ mV}$, $I_t = 0.1 \text{ nA}$) of SUC FeSe film prepared on the annealed anatase $\text{TiO}_2(001)$. (c) A series of dI/dV spectra (set point: $V_s = 50 \text{ mV}$, $I_t = 0.4 \text{ nA}$) acquired along the white arrow in b for every nanometer, revealing the almost identical superconducting gap magnitude ($\sim 17 \text{ meV}$). The spectra have been vertically shifted relative to each other by 0.2 for clarity.

$\sim 14 \text{ meV}$) in other heavily electron-doped FeSe-derived superconductors with no interfacial effect [19, 20], has recalled the crucial role of interfacial effects in the occurrence of high- T_c superconductivity. A direct comparison with SUC FeSe films on the $\text{SrTiO}_3(001)$ substrate with similar Δ can rule out both the interfacial tensile strain [4] and ferroelectric phonon screening [5] as the primacy for the enhanced superconductivity in terms of the very small lattice mismatch (0.9%) and dramatically different ferroelectric soft phonon frequency in the present case. On the other hand, the interaction between FeSe electrons and SrTiO_3 optical phonon at $\sim 100 \text{ meV}$ that has been proposed to be responsible for raising the superconductivity in SUC FeSe/ SrTiO_3 films [7, 9, 10] seems to work here: a nearly identical optical phonon does exist in anatase TiO_2 as well [32].

We now turn to study the charge transfer in the two heterostructures. It has been long believed that they are oxygen vacancies in the SrTiO_3 substrate that act as the source of electrons for the overlayer FeSe films [6, 14, 15]. However, it has not been vividly verified. Although the preparation of SrTiO_3 substrate and thus the density of oxygen vacancies might alter substantially among the samples from various groups, a direct relationship between the enhanced superconductivity and oxygen vacancies has never been established [1–4, 7]. To resolve this problem, we have employed STM to image oxygen vacancies and investigate their influence on superconductivity. As shown in Fig. 1(c), we can calculate easily the oxygen vacancy density to be $\sim 4.6 \times 10^{-2}$ per nm^2 ,

which even remains unchanged after the growth of FeSe films. This amount of vacancies (contributing ~ 0.013 electrons per Fe) is too small by nearly one order of magnitude to account for the necessary doping level of ~ 0.12 electrons per Fe for the occurrence of high- T_c superconductivity in SUC FeSe films [3], provided that an oxygen vacancy dopes two electrons into FeSe films. It thus suggests that the oxygen vacancies in TiO_2 may not be a sole source for electron doping in SUC FeSe films.

To understand this further, we have annealed the as-grown $\text{TiO}_2/\text{SrTiO}_3$ samples at 750°C to tune the density of oxygen vacancies and investigate their influence on the superconductivity. We find that a significant amount of oxygen atoms that desorb from SrTiO_3 can oxidize the overlayer TiO_2 islands. As shown in Fig. 3(a), it leads to an overall decrease in the density of oxygen vacancies to a level of 6.1×10^{-3} per nm^2 . However, on the $\text{TiO}_2(001)$ islands with significantly reduced surface oxygen vacancies (by nearly one order of magnitude), we observe no discernible change in both FeSe morphology [Fig. 3(b)] and superconducting gap magnitude Δ [Fig. 3(c)]. The results indicate that the surface oxygen vacancies in $\text{TiO}_2(001)$ may not be responsible mainly for the charge transfer and thus the high- T_c superconductivity in SUC FeSe films.

Other scenarios, such as interface element diffusion and band bending/alignment across the interface, may be responsible for the electron transfer between FeSe and anatase TiO_2 . According to Figs. 1(e) and 3(b), however, the FeSe/ TiO_2 interface is abrupt and there is no trace of substitution in FeSe films, indicating that the effect of interface diffusion is not significant. The work function of FeSe was recently measured to be larger than that of anatase TiO_2 [33]. Upon contact between FeSe and TiO_2 , the band alignment would lead to an electron transfer from TiO_2 to FeSe, consistent with our observation. As thus, the charge transfer mechanism in SUC FeSe/ TiO_2 might be caused by band alignment, which needs further confirmation in the future. Nevertheless, our direct comparison between TiO_2 and SrTiO_3 in this study further stresses the important role of interfacial electron-phonon coupling in the enhanced superconductivity in the two heterostructures.

This work is supported by the National Natural Science Foundation of China under Grant No. 10721404, 11134008 and 11504196, and the National Basic Research Program of China under Grant No. 2009CB929400. C. L. S. acknowledges support from the Tsinghua University Initiative Scientific Research Program.

* qkxue@mail.tsinghua.edu.cn

[1] Q. Y. Wang, Z. Li, W. H. Zhang, Z. C. Zhang, J. S. Zhang, W. Li, H. Ding, Y. B. Ou, P. Deng, K. Cahng,

- J. Wen, C. L. Song, K. He, J. F. Jia, S. H. Ji, Y. Y. Wang, L. L. Wang, X. Chen, X. C. Ma, and Q. K. Xue, *Chin. Phys. Lett.* **29**, 037402 (2012).
- [2] D. F. Liu, W. H. Zhang, D. X. Mou, J. F. He, Y. B. Ou, Q. Y. Wang, Z. Li, L. L. Wang, L. Zhao, S. L. He, Y. Y. Peng, X. Liu, X. Y. Chen, L. Yu, G. D. Liu, X. L. Dong, J. Zhang, C. T. Chen, Z. Y. Xue, J. P. Hu, X. Chen, X. C. Ma, Q. K. Xue, and X. J. Zhou, *Nat. Commun.* **3**, 931 (2012).
- [3] S. L. He, J. F. He, W. H. Zhang, L. Zhao, D. F. Liu, X. Liu, D. X. Mou, Y. B. Ou, Q. Y. Wang, Z. Li, L. L. Wang, Y. Y. Peng, Y. Liu, C. Y. Chen, L. Yu, G. D. Liu, X. L. Dong, J. Zhang, C. T. Chen, Z. Y. Xu, X. Chen, X. C. Ma, Q. K. Xue, and X. J. Zhou, *Nat. Mater.* **12**, 605 (2013).
- [4] S. Y. Tan, Y. Zhang, M. Xia, Z. R. Ye, F. Chen, X. Xie, R. Peng, D. F. Xu, Q. Fan, H. C. Xu, J. Jiang, T. Zhang, X. C. Lai, T. Xiang, J. P. Hu, N. P. Xie, and D. L. Feng, *Nat. Mater.* **12**, 634 (2013).
- [5] Y. Y. Xiang, F. Wang, D. Wang, Q. H. Wang, and D. H. Lee, *Phys. Rev. B* **86**, 134508 (2012).
- [6] J. Bang, Z. Li, Y. Y. Sun, A. Samanta, Y. Y. Zhang, W. H. Zhang, L. Wang, X. Chen, X. C. Ma, Q. K. Xue, and S. B. Zhang, *Phys. Rev. B* **87**, 220503 (2013).
- [7] J. J. Lee, F. T. Schmitt, R. G. Moore, S. Johnston, Y. T. Cui, W. Li, M. Yi, Z. K. Liu, M. Hashimoto, Y. Zhang, D. H. Lu, T. P. Devereaux, D. H. Lee, and Z. X. Shen, *Nature* **515**, 245 (2014).
- [8] Y. Miyata, K. Nakayama, K. Sugawara, T. Sato, and T. Takahashi, *Nat. Mater.* **14**, 775 (2015).
- [9] L. Rademaker, Y. Wang, T. Berlijn, and S. Johnston, *arXiv preprint arXiv:1507.03967* **18**, 022001 (2016).
- [10] Z. X. Li, F. Wang, H. Yao, and D. H. Lee, *arXiv preprint arXiv:1512.06179* (2015).
- [11] K. Nakayama, Y. Miyata, G. Phan, T. Sato, Y. Tanabe, T. Urata, K. Tanigaki, and T. Takahashi, *Phys. Rev. Lett.* **113**, 237001 (2014).
- [12] C. L. Song, Y. L. Wang, P. Cheng, Y. P. Jiang, W. Li, T. Zhang, Z. Li, K. He, L. Wang, J. F. Jia, H.-H. Hung, C. J. Wu, X. C. Ma, X. Chen, and Q. K. Xue, *Science* **332**, 1410 (2011).
- [13] R. Peng, H. C. Xu, S. Y. Tan, H. Y. Cao, M. Xia, X. P. Shen, Z. C. Huang, C. H. P. Wen, Q. Song, T. Zhang, B. P. Zie, and D. L. Feng, *Nat. Commun.* **5**, 5044 (2014).
- [14] G. Y. Zhou, D. Zhang, C. Liu, C. J. Tang, X. Wang, Z. Li, C. Song, S. Ji, K. He, L. Wang, X. C. Ma, and Q. K. Xue, *Appl. Phys. Lett.* **108**, 202603 (2016).
- [15] P. Zhang, X. L. Peng, T. Qian, P. Richard, X. Shi, J.-Z. Ma, B.-B. Fu, Y. L. Guo, Z. Q. Han, S. C. Wang, L. L. Wang, Q. K. Xue, J. P. Hu, Y. J. Sun, and H. Ding, *arXiv preprint arXiv:1512.01949* (2015).
- [16] M. Burrard-Lucas, D. G. Free, S. J. Sedlmaier, J. D. Wright, S. J. Cassidy, Y. Hara, A. J. Corkett, T. Lancaster, P. J. Baker, S. J. Blundell, and S. J. Clarke, *Nat. Mater.* **12**, 15 (2013).
- [17] X. F. Lu, N. Z. Wang, H. Wu, Y. P. Wu, D. Zhao, X. Z. Zeng, X. G. Luo, T. Wu, W. Bao, G. H. Zhang, and X. H. Chen, *Nat. Mater.* **14**, 325 (2015).
- [18] B. Lei, J. H. Cui, Z. J. Xiang, C. Shang, N. Z. Wang, G. J. Ye, X. G. Luo, T. Wu, Z. Sun, and X. H. Chen, *Phys. Rev. Lett.* **116**, 077002 (2016).
- [19] C. L. Song, H. M. Zhang, Y. Zhong, X. P. Hu, S. H. Ji, L. Wang, K. He, X. C. Ma, and Q. K. Xue, *Phys. Rev. Lett.* **116**, 157001 (2016).
- [20] Y. Zhang, J. J. Lee, R. G. Moore, W. Li, M. Yi, M. Hashimoto, D. H. Lu, T. P. Devereaux, D. H. Lee, and Z. X. Shen, *arXiv preprint arXiv:1512.06322* (2015).
- [21] M. Mikami, S. Nakamura, O. Kitao, and H. Arakawa, *Phys. Rev. B* **66**, 155213 (2002).
- [22] Y. Wang, H. Sun, S. Tan, H. Feng, Z. Cheng, J. Zhao, A. Zhao, B. Wang, Y. Luo, J. L. Yang, and J. G. Hou, *Nat. Commun.* **4**, 2214 (2013).
- [23] Q. Fan, W. H. Zhang, X. Liu, Y. J. Yan, M. Q. Ren, R. Peng, H. C. Xu, B. P. Xie, J. P. Hu, T. Zhang, and D. L. Feng, *Nat. Phys.* **11**, 946 (2015).
- [24] Y. De Wilde, M. Iavarone, U. Welp, V. Metlushko, A. E. Koshelev, I. Aranson, G. W. Crabtree, and P. C. Canfield, *Phys. Rev. Lett.* **78**, 4273 (1997).
- [25] N. Nakai, P. Miranović, M. Ichioka, and K. Machida, *Phys. Rev. Lett.* **89**, 237004 (2002).
- [26] S. P. Brown, D. Charalambous, E. C. Jones, E. M. Forgan, P. G. Kealey, A. Erb, and J. Kohlbrecher, *Phys. Rev. Lett.* **92**, 067004 (2004).
- [27] H. Sakata, M. Oosawa, K. Matsuba, N. Nishida, H. Takeya, and K. Hirata, *Phys. Rev. Lett.* **84**, 1583 (2000).
- [28] R. Gilardi, J. Mesot, A. Drew, U. Divakar, S. L. Lee, E. M. Forgan, O. Zaharko, K. Conder, V. K. Aswal, C. D. Dewhurst, R. Cubitt, N. Momono, and M. Oda, *Phys. Rev. Lett.* **88**, 217003 (2002).
- [29] B. B. Zhou, S. Misra, E. H. da Silva Neto, P. Aynajian, R. E. Baumbach, J. Thompson, E. D. Bauer, and A. Yazdani, *Nature Physics* **9**, 474 (2013).
- [30] N. Nakai, P. Miranović, M. Ichioka, and K. Machida, *Phys. Rev. Lett.* **89**, 237004 (2002).
- [31] N. Hayashi, T. Isoshima, M. Ichioka, and K. Machida, *Phys. Rev. Lett.* **80**, 2921 (1998).
- [32] S. Moser, L. Moreschini, J. Jaćimović, O. S. Barišić, H. Berger, A. Magrez, Y. J. Chang, K. S. Kim, A. Bostwick, E. Rotenberg, L. Forró, and M. Grioni, *Phys. Rev. Lett.* **110**, 196403 (2013).
- [33] P. Jiang, private communication.